Colloid Polym Sci (2008) 286:1273–1280
DOI 10.1007/s00396-008-1891-1

ORIGINAL CONTRIBUTION

Influence of emulsification process on structure–properties relationship of highly concentrated reverse emulsion-derived materials

Olivier Lépine · Marc Birot · Hervé Deleuze

Received: 13 February 2008 / Revised: 19 May 2008 / Accepted: 20 May 2008 / Published online: 16 June 2008

Abstract Water-in-Oil high internal phase emulsions (HIPEs) whose continuous phase is polymerizable gave access to highly porous polymeric materials (polyHIPEs). These emulsions were prepared with a laboratory-made homogenizer whose shear frequency and time could be varied to study the influence of the emulsification conditions on the polyHIPEs morphology. Intensive and/or long shear induced a reduction of the cell and connection diameters without any modification of the material global porosity. The mechanical properties were evaluated by estimating the Young's modulus from compression tests. The mechanical behavior was analogous for all materials possessing a characteristic polyHIPE structure, even if cell sizes were different between samples.

Keywords PolyHIPE · Emulsification · Cellular polymer · Highly concentrated emulsion

Introduction

An emulsion is a two-liquid mixture thermodynamically instable by nature, evolving spontaneously to phase separation. The unfavorable emulsion state can be obtained by an energy supply to the system, which is generally brought by mechanical mixing [1]. The range of emulsification devices is very broad: mechanical stirring systems, colloidal mills, high-pressure homogenizers, ultrasound homogenizers, porous membranes [1–4]. The type of mixing system employed influences strongly the droplets size of the dispersed phase.

Particular emulsions with a high volume fraction of dispersed phase are described in the literature and allow access to highly porous materials. Such polymers are known in the literature for many years as polyHIPEs [5] and have found an increasing number of applications: absorbents for liquids [6, 7], supports for organic synthesis [8–11], scavengers [12], aerosol filtration media [13–15], insulation materials [16], scaffolds for cell growth [17–21]. These materials, initially developed by Unilever [22], are obtained by polymerization of a highly concentrated emulsion, or high internal phase emulsion (HIPE), resulting from the surfactant stabilized dispersion of a large volume of internal phase (or dispersed phase) in a continuous phase (or monomeric phase). While increasing the volume of the dispersed phase beyond 74%, the water droplets tend to deform into polyhedra surrounded by a thin film of continuous phase [5, 23].

As the polyHIPE porous structure is directly derived from the starting concentrated emulsion morphology, the emulsion preparation conditions will strongly influence the cellular morphology of the final material [22, 24–30]. However, solely a limited number of works has been devoted, so far, to the study of the influence of emulsification conditions on the morphology of polyHIPE materials. In this area, HIPEs are generally obtained by progressive addition of an aqueous phase into an organic phase under mechanical stirring without any control of the parameters involved [23, 31]. Few authors investigated other emulsification processes. At an industrial scale, homogenizers are commonly used emulsification equipments. A homogenizer is a device with which dispersion is realized by forcing the mixture to be emulsified through a

O. Lépine · M. Birot · H. Deleuze (✉)
Institut des Sciences Moléculaires (ISM), Université Bordeaux I,
CNRS UMR 5255,
351 Cours de la Libération,
33405 Talence Cedex, France
e-mail: h.deleuze@ism.u-bordeaux1.fr

small orifice under very high pressure. These apparatus are very efficient but not adapted to laboratory-scale experiments. In an early study, Becher developed a homogenizer designed for small-scale laboratory preparation in which two hypodermic syringes were linked by a small tube, through which the liquids to be emulsified passed back and forth by alternative air pressure admission on the plungers [32]. By using design of experiments, Becher put into evidence that the dispersed phase droplets average diameter and standard deviation of concentrated oil-in-water emulsions were strongly influenced by three experimental parameters: the number of passes through the connecting tube, the air pressure, and the connecting tube diameter. More recently, Kong related the preparation of low-density carbonized composite foams derived from inverse emulsions of styrene/divinylbenzene mixtures in water obtained using a similar device [33]. The authors claimed materials with connected cells of 1–2 μm in diameter, but no experimental details were displayed.

In this paper, we prepared a range of HIPEs based on the monomers system the most commonly used (styrene-divinylbenzene) [21, 22, 26, 31, 34, 35], while using a Becher-like homogenizer. In our device, the reciprocal action was actuated by an electric motor.

We investigated the influence of the motor speed and emulsification time on the porous structure characteristics of the resulting polyHIPEs.

Experimental part

Materials

Styrene (stabilized, p.a.) and sodium chloride (p.a.) were purchased from Acros Organics and used as received. Divinylbenzene (technical, 80% DVB+20% ethylstyrene, mixture of isomers), potassium persulphate (99%+, A.C.S. reagent) and sorbitan monooleate (Span®80) were purchased from Aldrich and used as supplied.

Determination of macroporosity

The porosity and pore size distribution of each sample were determined by mercury intrusion porosimetry using a Micromeritics Autopore IV 9500 instrument.

Surface area and mesoporosity measurements

The specific surface area was determined by N_2 adsorption measurements performed on a Micromeritics ASAP 2010. The resulting data were subjected to the Brunauer, Emmet and Teller (BET) [36] or the Barrett, Joyner and Halenda (BJH) [37] treatments.

Electron microscopy investigations

The morphology of the monoliths was observed by scanning electron microscopy (SEM) on a Jeol JSM 5200 microscope. The photographs were taken at several different magnifications between ×1,000 and ×20,000. Pieces of polyHIPEs (section of about 0.5 cm^2) cut from the corresponding monoliths were mounted on a copper stub, which ensured a good conductivity. A thin layer of gold was sputtered on the polyHIPE fragment prior to analysis.

An average cell diameter (ϕ_{cell}) was estimated for each sample from SEM micrographs after image processing with Scion Image freeware (Scion Corporation, Frederick, MD, USA, http://www.scioncorp.com/). The mean and the standard deviation were drawn by manual measurements of diameters from a population of at least 150 cells. To get a better estimation of the real cell diameter, a statistical correction [38] was introduced by multiplying the observed average value by a factor $K=2/(3^{1/2})$.

Mechanical analysis

Compression tests were carried out at room temperature on an Instron 4460 testing machine with a static loading cell of 500 N. Cylindrical samples (diameter=7 mm, thickness=4 mm) were compressed at constant speed rate (5 mm min^{-1}) on their flat surfaces between metallic plates. The mean and the standard deviation of the Young's modulus E_c were calculated from the data obtained with seven samples of the same composition.

Emulsification system

Emulsification was performed using a laboratory-made system composed of two polyethylene syringes (50 mL, internal diameter=28 mm) connected with a small-section tube (nylon, ID=11 mm, OD=4 mm, length=20 mm). The components of the emulsion (about 20 mL) were put into one of the syringes and the emulsion was formed by successive passages through the tube produced by the backwards and forwards motion of the syringe plungers. The rate of passage of the emulsion through the connecting tube was controlled by adjusting the power frequency of the electric motor used (Fig. 1).

HIPE preparation and polymerization

The continuous phase was composed of the comonomers and the surfactant (20 wt.% of the continuous phase). The aqueous phase represented 80 wt.% of the total weight of the emulsion and was constituted of distilled water, sodium chloride (2 wt.%) and potassium persulphate as radical initiator (2 wt.%).

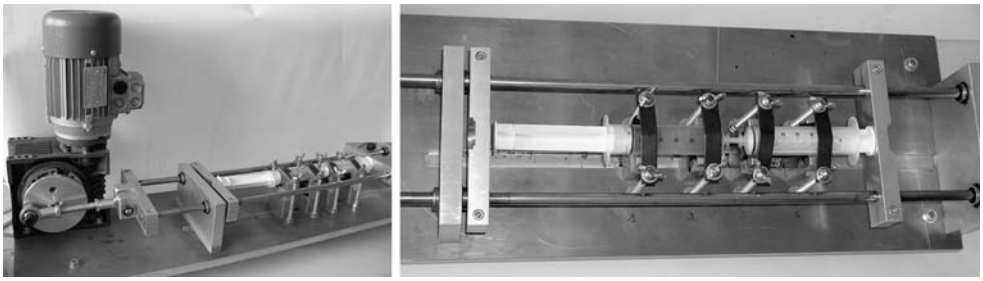

Fig. 1 Laboratory-made syringe pump device used for highly concentrated reverse emulsion generation

Both phases were put into a 50-mL syringe and intimately mixed with the previously described emulsification system. The emulsion thus obtained was then placed in a PTFE cylindrical mould (internal diameter=15 mm; height=16 mm) and polymerized for 24 h at 60 °C in an oven. The resulting polyHIPE monoliths were extracted by refluxing an ethanol/water (50:50 *v*/*v*) mixture in a Soxhlet apparatus (24 h) and dried in a vacuum oven at room temperature.

Results and discussion

Preparation of poly(styrene-*co*-divinylbenzene) polyHIPEs

poly(styrene-*co*-divinylbenzene) (PS) polyHIPEs were prepared from an equimolar styrene-divinylbenzene mixture (organic phase) and an aqueous dispersed phase representing 80% of the total emulsion volume. These phases were intimately mixed using the previously described syringe pump device. Different values of shear time (t_{shear}) and transfer rate (number of emulsion transfers from one syringe to the other per minute, expressed as the shear frequency f_{shear}) were used in order to study the influence of such modifications on the material cellular structure. The connecting tube diameter was kept constant throughout the study (Table 1).

The emulsification conditions did not affect the emulsion stability: all generated emulsions were perfectly stable for at least seven consecutive days. The emulsions were then cured (polymerization, extraction, and drying) to obtain polyHIPEs. Effects of emulsification conditions on the cellular morphology were investigated by SEM, mercury porosimetry, and nitrogen adsorption. The droplets size of concentrated emulsions is difficult to estimate directly. However, as mentioned already, its evolution can reasonably be correlated to the observed cells diameter behavior in the corresponding final material.

Table 1 Emulsification conditions for high concentrated reverse emulsion prepared with the syringe pump device

Sample	S1	S2	S3	S4	S5	S6	S7	S8	S9
t_{shear} (min)	35	35	35	35	2	15	60	90	300
f_{shear} (min^{-1})	14	18	22	27	14	14	14	14	14

Influence of shear frequency on cellular microstructure

SEM was used to investigate the presence of the characteristic porous structure of polyHIPEs. SEM micrographs of samples S1–4 are presented in Fig. 2. A connected cellular morphology was observed, whatever the conditions employed for the emulsions production. A shear frequency increase induced a decrease in the cells diameter. In all materials, the dispersion of cells diameter appeared relatively narrow and so, independent of the shear frequency used for emulsification.

To quantify these visual observations, an average cell diameter (ϕ_{cell}) was evaluated for each sample from SEM micrographs and reported, with the corresponding standard deviation ($\sigma(\phi_{cell})$), in Table 2. Mercury porosimetry and nitrogen adsorption measurements were also reported in this Table.

Firstly, it can be noted that a modification in the emulsification conditions did not affect the final porosity of the materials. As the expected porosity of a polyHIPE is determined by the volume fraction of the dispersed phase introduced into the emulsion before polymerization, this observation confirms the high stability of all the emulsions prepared.

The previous observation concerning the evolution of the cells diameter with the shear frequency was confirmed: ϕcell decreased from 2.5 to 0.9 μm with progressive increase of f_{shear} (Fig. 3a). This evolution can be explained by the progressive increase of the Laplace's force when the droplets diameter decreases. In others words, the smallest the droplets are, the strongest the Laplace's force is and so, the more difficult the later breaking up of the droplets will be [1].

The connections size distribution of the monoliths derived from the emulsions prepared with a low shear frequency is rather narrow and centered on 537 nm (S1, Table 2). When the shear rate was increased, the connections diameter shifted toward smaller values (maximum at 335 nm for S2 to 171 nm for S4). Its distribution widened and a second connection class appeared at higher diameters (250–600 nm) with a larger distribution than the first one (Fig. 3).

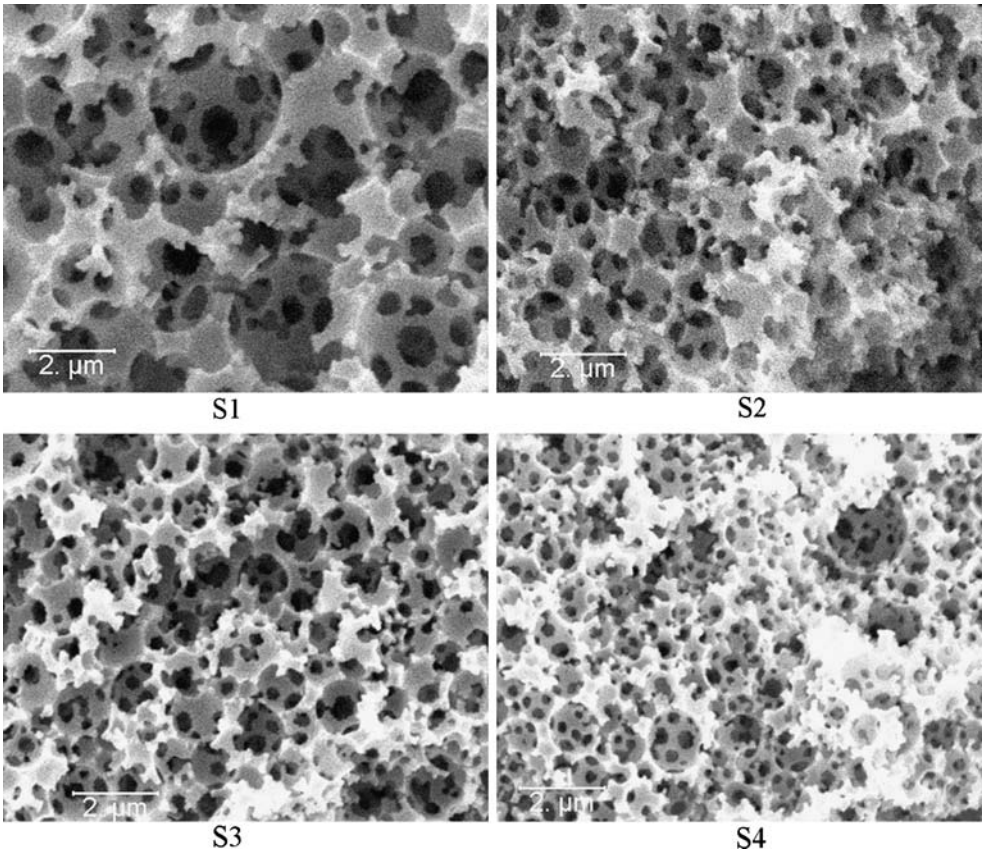

Fig. 2 ×10,000 SEM micrographs of PS polyHIPEs obtained from emulsions elaborated with increasing shear frequencies

The phenomenon involved in the generation of the connections between cells is still under debate. The most commonly assumed mechanism concerns the drainage of the organic phase components and the polymer contraction during the polymerization step. Connections are created by film tearing where the polymer is the thinnest, i.e., where the water droplets are the closest. Barby and Haq [22] attributed the formation of connections to the surfactant that is excluded from the two emulsion phases during polymerization. The subsequent extraction step will clean the surfactant molecules out of the material, creating voids between adjacent cells. Williams and Wrobleski [29] noted a modification of the porous structure with the surfactant concentration. According to the authors, a concentration increase induces a thinning of the monomer film surrounding the water droplets, making easier the formation of bigger connections. However, in a recent paper, Menner and Bismarck stated that the formation of the connections is caused by the mechanical rupture of the polymer film covering the faces between droplets [39].

As formation of connections occurs during the polymerization step, variations of their size cannot be directly attributed to the emulsification process. However, the connections size decrease can be correlated, to some extent, to the observed cells diameter decrease in the final material when the shear frequency is increased during the emulsion

Table 2 Influence of shear frequency on cellular morphology of porous PS elaborated from highly concentrated reverse emulsions

Sample[a]	f_{shear}[b] (min^{-1})	ϕ_{cell}[c] (µm)	$\sigma(\phi_{cell})$[c] (µm)	Porosity[d] (%)	$\phi_{connections}$[d] (nm)	Surface area[e] ($m^2.g^{-1}$)	$\phi_{mesopores}$[f] (nm)
S1	14	2.5	0.7	81	537	11	7
S2	18	1.6	0.3	83	335	16	7
S3	22	1.3	0.3	83	240	19	7
S4	27	0.9	0.2	83	171	27	9

[a] 80% of dispersed aqueous phase, t_{shear}=35 min
[b] Shear frequency, number of emulsion transfers from one syringe to the other per minute
[c] Estimated from SEM micrographs
[d] Determined by mercury porosimetry; $\phi_{connections}$=connection diameter at the maximum of the distribution curve
[e] Calculated from nitrogen adsorption measurements subjected to the BET treatment
[f] Calculated from nitrogen adsorption measurements subjected to the BJH treatment

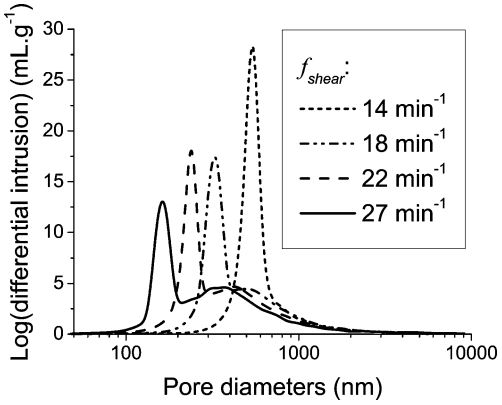

Fig. 3 Evolution of connections diameter distribution with shear frequency

preparation. Thus, for a given emulsion volume, the formation of smaller water droplets induces an increase of the total number of droplets (correlated with an increase of the total surface area of the droplets). Therefore, the surfactant layer surrounding small droplets is thinner than in the case of larger ones, thus allowing the formation of more numerous, and therefore smaller connections.

Similarly, the connections size distribution widening with the shear frequency increasing can be correlated to a less homogeneous cells size distribution. Becher [32] noted that an excessive shear induced an increase in the emulsion particles size. The droplets of the dispersed phase can be partially destabilized, due to a too important energy supply, contributing to bigger cells and a broadening of the cells distribution [1, 40].

Nitrogen adsorption measurements presented a small increase in the surface area with increasing shear frequencies, which tended to indicate the creation of some mesoporosity (11 $m^2.g^{-1}$ for S1, 27 $m^2.g^{-1}$ for S4). On the other hand, no noticeable modification in the mesopores diameter was observed (7–9 nm).

Influence of the shear time on cellular microstructure

We prepared a range of emulsions with a constant shear frequency (f_{shear}=14 min^{-1}), but with increasing shear time (t_{shear} from 2 to 300 min). The materials obtained after polymerization of the emulsions presented a narrow connections diameter distribution.

Shear time influenced the emulsion structure and, consequently, that of the resulting porous polymer. SEM micrographs study indicated a decrease in the cells size with increasing shear times (S6 to S9). For short shear time (S5), a very particular porous structure was obtained: the cells presented very large connections delimited by polymer beams corresponding to the edges shared between adjacent cells, called plateau borders. In that case, the starting emulsion appeared much less viscous (liquid) than in other cases. Because of its low viscosity, the organic phase surrounding the water droplets could move easily from the films separating two cells to the shared edges: this phenomenon is described in the literature as liquid drainage [41–45].

Due to its particular porous structure, no cells diameter measurements were made for sample S5. For all other samples, an average cell diameter was determined and reported in Table 3.

The experimental material porosity values were found to be as expected in any case. Mercury porosimetry measurements results confirmed the decrease in the cells diameter with the increase of the number of passes, as observed by SEM (Fig. 4). Similarly, a decrease in the connections size was observed as the shear time was increased. A quite narrow cells size distribution curve was obtained with a maximum peak ($\phi_{connection}$) shifting from 1,300 to 300 nm as t_{shear} increased from 2 to 300 min. Except for S5, surface areas and mesopores diameters were quite similar whatever the shear time: 12–15 m^2 g^{-1} and 7–10 nm respectively [31, 34]. Due to its particular porous structure, S5 presented a

Table 3 Influence of shear time on cellular morphology of porous PS elaborated from highly concentrated reverse emulsions

Sample[a]	t_{shear}[b] (min)	ϕ_{cell}[c] (μm)	σ(ϕ_{cell})[c] (μm)	Porosity[d] (%)	$\phi_{connections}$[d] (nm)	Surface area[e] ($m^2.g^{-1}$)	$\phi_{mesopores}$[f] (nm)
S5	2	–	–	81	1361	27	13
S6	15	3.0	0.7	81	768	12	10
S1	35	2.5	0.7	81	537	11	7
S7	60	2.1	0.6	82	542	17	9
S8	90	1.7	0.7	83	433	14	8
S9	300	1.5	0.6	84	304	14	7

[a] 80% of dispersed aqueous phase, f_{shear}=14 min^{-1}
[b] Shear time
[c] Estimated from SEM micrographs
[d] Determined by mercury porosimetry; $\phi_{connection}$=connections diameter at the maximum of the distribution curve
[e] Calculated from nitrogen adsorption measurements subjected to the BET treatment
[f] Calculated from nitrogen adsorption measurements subjected to the BJH treatment

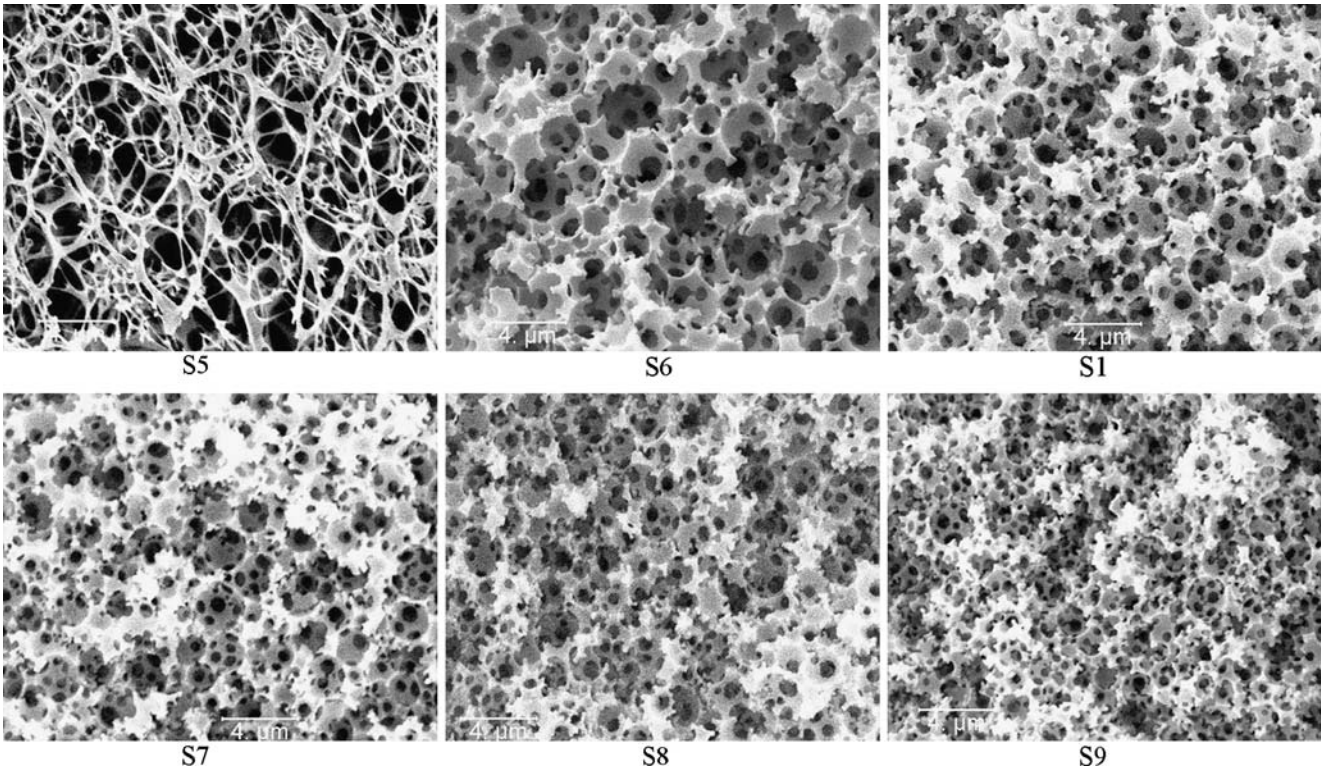

Fig. 4 ×5,000 SEM micrographs of PS polyHIPEs obtained from emulsions elaborated with increasing shear times

specific surface area twice as high as did other materials exhibiting a "classical" polyHIPE structure (S1, S6–9).

Figure 5 reports the evolution of the connections size distribution with the shear time as estimated by mercury porosimetry. This distribution widened, but the second diameter population appeared only after very long shear time.

Compared effects of shear frequency and shear time

Shear frequency and shear time modifications presented similar effects on the porous structure of the final solid materials and, therefore, presumably on the starting emulsions structure. However, the intensity of these effects was different. Shear frequencies and shear times can both be converted into number of passes of the emulsion components through the connecting tube (N_{pass}). The evolution of the average cells size with N_{pass} is reported in Fig. 6.

The modifications of the cells diameter were more pronounced when the shear frequency increased than when the shear time was extended. As an example, a cells diameter of 1.3 μm could be observed from an emulsion obtained after 35-min-mixing with a shear frequency of 22 min^{-1} (S3), whereas, with a lower f_{shear} value

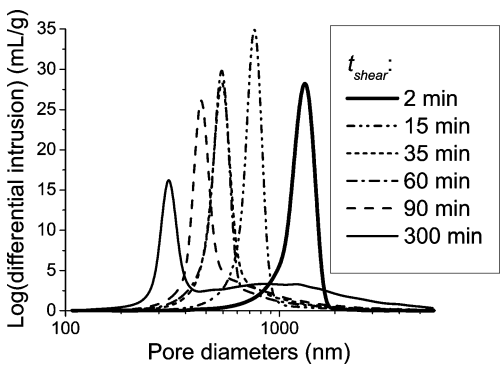

Fig. 5 Evolution of connections diameter distribution with shear time

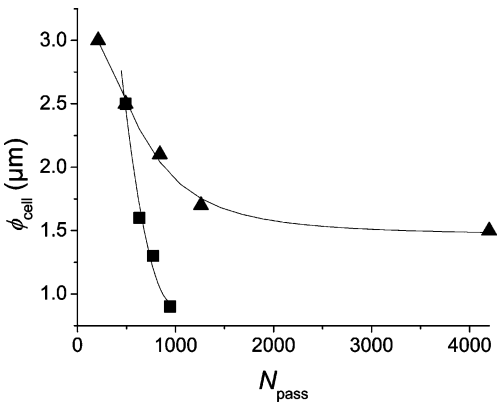

Fig. 6 Compared effects of shear frequency (*filled square*) and shear time (*filled diamond*) as expressed in pass number (N_{pass}) on average cells diameter

Table 4 Young's moduli of highly porous materials obtained by polymerization of emulsion elaborated with various shear conditions

Sample	E_c (MPa)	$\sigma(E_c)$ (MPa)
S1	19.5	3.5
S2	22.0	4.0
S4	25.0	2.5
S5	40.0	6.0
S6	27.5	5.0
S7	23.5	3.5
S8	19.5	3.5
S9	19.0	3.0

(14 min^{-1}), the shear time had to be increased up to 300 min (S9) to obtain the same result.

The mechanisms involved in the droplets generation are various and depend on the dispersed phase velocity [1], which is function of the pressure applied to force the emulsion components to migrate from one syringe to the other. In the device employed, it corresponds to the shear frequency. The connections diameter was less well-controlled and its distribution tended to become more complex with a variation of shear frequency, whereas these observations were only done for very long shear times (S9, t_{shear}=300 min). In other words, the HIPE stability was much more affected by a variation in f_{shear} than in t_{shear}.

Porous structure-mechanical properties relationship in polyHIPEs

The mechanical behavior of the obtained highly porous materials was evaluated by measurements of their resistance to compression at ambient temperature. Elastic moduli, or Young's moduli E_c, were determined from the corresponding stress–strain curves by using the Hooke's law. For each sample, the mean E_c and the standard deviation $\sigma(E_c)$ are reported in Table 4.

Except for S5, the E_c values were in the range of 20–27 MPa with standard deviations of about 3–5 MPa. It was demonstrated that, for a network of model cells, the Young's modulus of a cellular material with open cells is given by the relation [46]:

$$E = \frac{\sigma}{\varepsilon} = C_1 \cdot E_S \cdot \left(\frac{\rho}{\rho_S}\right)^2$$

E, ρ are the Young's modulus and the bulk density of the porous material and E_S, ρ_S the modulus and the skeleton density of the solid, respectively. C_1 is a coefficient including various proportional geometric constants (geometric order of cells, stacking uniformity, and cell walls curvature…). Consequently, the mechanical properties of cellular materials depend on their composition, their density and the geometry of their internal structure.

The different polyHIPE samples prepared have the same formulation and so, the same E_S and ρ_S values. As ρ values (drawn from mercury intrusion analyses) appeared similar for all samples, the little variations in E_c values can be attributed to the modifications of the porous structure (cells and/or connections diameter), inducing a variation of the C_1 parameter.

The peculiar porous structure of S5 observed in Fig. 4 caused a more pronounced variation of the Young's modulus value compared to others samples: E_S of the "beam structure" material being significantly higher than those of materials with microcellular morphology are. This higher rigidity of S5 can be explained by a higher concentration of the polymer into the beams, conducing to a higher resistance to compression. Inversely, the porous structures of S1–4 and S6–9 were composed of cells surrounded by thin polymer films inducing a higher flexibility.

The Young's modulus standard deviation values decreased while the number of passes through the connecting tube increased: $\sigma(E_c)$ was slightly higher for S5 and S6 than for S1–4 and S7–9 samples. Such a variation indicates a progressive narrowing in the water droplets diameter distribution, therefore in cells diameter, when the number of passes increased.

Conclusions

In this work, we have shown that the use of a laboratory-scale homogenizer for the preparation of highly concentrated reverse emulsions allowed an easy control of the morphology on the resulting polyHIPE materials. We hope that the use of this device will allow increasing the knowledge about the transformation of an emulsion into a rigid material.

Acknowledgements This work was supported by the Agence Nationale de la Recherche (funding and grant for OL).

References

1. Dalmazzone C (2000) Oil Gas Sci Technol-Rev IFP 55:281
2. Charcosset C, Limayem I, Fessi H (2004) J Chem Technol Biotechnol 79:209
3. Tadros T, Izquierdo P, Esquena J, Solans C (2007) Adv Colloid Interface Sci 108–109:303
4. Alban B, Canselier J-P, Le Sauze N, Poux M, Xuereb C (2003) STP Pharma Pratiques 13:16
5. Lissant, KJ (1974) Emulsions and emulsion technology-part I. Marcel Dekker Inc., New York, NJ
6. Conrad JP, Dyer JC, Hortel TC, Westendorf RD (2001) US Patent 6245697 to the Procter & Gamble Company CA 132: 348693 (2000)

7. Dyer JC, DesMarais TA, LaVon GD, Stone KJ, Taylor GW, Young GA (1995) US Patent 5387207 to the Procter & Gamble Company CA 122: 267419 (1995)
8. Hird N, Hughes I, Hunter D, Morrisson MGJT Sherrington DC, Stevenson, L (1999) Tetrahedron 55:9575
9. Cetinkaya S, Khosravi E, Thompson R (2006) J Mol Catal A 254:138
10. Deleuze H, Maillard B, Mondain-Monval O (2002) Bioorg Med Chem Lett 12:1877
11. Mercier A, Deleuze H, Mondain-Monval O (2000) React Funct Polym 46:67
12. Krajnc P, Brown JF, Cameron NR (2002) Org Lett 4:2497
13. Bhumgara Z (1995) Filtr Sep 32:245
14. Bhumgara ZG (1995) A study of the development of polyHIPE foam material for use in separation processes. PhD Thesis, University of Exeter (UK)
15. Walsh, DC Stenhouse JIT, Kingsbury LP, Webster EJ (1996) J Aerosol Sci 27:S629
16. Dyer JC, DesMarais TA (1997) US Patent 5633291 to the Procter & Gamble Company CA 126: 118822 (1997)
17. Bokhari MA, Birch MA, Akay G (2003) Adv Exp Med Biol 534:247
18. Busby W, Cameron NR, Jahoda CA (2001) Biomacromolecules 2:154
19. Barbetta, A, Dentini, M, Zannoni, EM, De Stefano, ME (2005) Langmuir 21:12333
20. Hayman MW, Smith KH, Cameron NR, Przyborski SA (2004) Biochem Biophys Res Commun 314:483
21. Hough DB, Hammmond K, Morris C, Hammond RC (1991) US Patent 5071747 to Unilever CA 112:72946 (1990)
22. Barby D, Haq Z (1982) European Patent 0,060,138 to Unilever CA 98: 5252 (1983)
23. Cameron, NR, Sherrington, DC (1996) Adv Polym Sci 126:163
24. Aronson MP, Petko MF (1986) US Patent 4606913 to Lever Brothers Company CA 98: 145908 (1983)
25. Chen HH, Ruckenstein E (1991) J Colloid Interface Sci 145:260
26. Krajnc P (2002) Polimery 47:26
27. Kunieda H, Yano N, Solans C (1989) Colloids Surf 36:313
28. Solans C, Azemar N, Parra, JL (1988) Prog Colloid Polym Sci 76:224
29. Williams JM, Wrobleski DA (1988) Langmuir 4:656
30. Carnachan RJ, Bokhari M, Przyborski SA, Cameron NR (2006) Soft Matter 2:608
31. Cameron NR (2003) J Chromatogr Libr 67:255
32. Becher, P (1967) J Colloid Interface Sci 24:91
33. Kong FM (1991) US Patent 5047225 to the United States of America CA 115: 160929 (1991)
34. Hainey P, Huxham IM, Rowatt B, Sherrington DC, Tetley L (1991) Macromolecules 24:117
35. Williams JM, Gray AJ, Wilkerson MH (1990) Langmuir 6:437
36. Brunauer S, Emmet PH, Teller E (1938) J Am Chem Soc 60:309
37. Barrett EP, Joyner LG, Halenda PP (1951) J Am Chem Soc 73:373
38. Barbetta A, Cameron, NR (2004) Macromolecules 37:3188
39. Menner A, Bismarck A (2006) Macromol Symp 242:19
40. Chen G, Tao D (2005) Fuel Process Technol 86:499
41. Bhakta A, Ruckenstein E (1997) J Colloid Interface Sci 191:184
42. Nguyen, AV (2002) J Colloid Interface Sci 249:194
43. Narsimhan G (1991) J Food Eng 14:139
44. Ramani MV, Kumar R, Gandhi KS (1993) Chem Eng Sci 48:455
45. Podual K, Kumar R, Gandhi KS (1996) Chem Eng Sci 51:1393
46. Gibson LJ, Ashby MF (2001) Cellular solids. Structure and properties. Cambridge University Press, Cambridge (UK)